Received: 25 November 2019 | Revised: 13 March 2020 | Accepted: 14 March 2020

DOI: 10.1002/hbm.24999

WILEY

RESEARCH ARTICLE

Effective brain connectivity at rest is associated with choice-induced preference formation

Katharina Voigt[1,2] | Carsten Murawski[3] | Sebastian Speer[1,4] | Stefan Bode[1,5]

[1]Melbourne School of Psychological Sciences, The University of Melbourne, Carlton, Victoria, Australia

[2]School of Psychological Sciences and Turner Institute for Brain and Mental Health, Monash University, Clayton, Victoria, Australia

[3]Department of Finance, The University of Melbourne, Carlton, Victoria, Australia

[4]Rotterdam School of Management, Erasmus University, Rotterdam, The Netherlands

[5]Department of Psychology, University of Cologne, Cologne, Germany

Correspondence
Stefan Bode, Melbourne School of Psychological Sciences, The University of Melbourne, Redmond-Barry Building, Parkville, VIC 3010, Australia.
Email: sbode@unimelb.edu.au

Abstract

Preferences can change as a consequence of making a hard decision whereby the value of chosen options increases and the value of rejected options decreases. Such choice-induced preference changes have been associated with brain areas detecting choice conflict (anterior cingulate cortex, ACC), updating stimulus value (dorsolateral prefrontal cortex, dlPFC) and supporting memory of stimulus value (hippocampus and ventromedial prefrontal cortex, vmPFC). Here we investigated whether resting-state neuronal activity within these regions is associated with the magnitude of individuals' preference updates. We fitted a dynamic causal model (DCM) to resting-state neuronal activity in the spectral domain (spDCM) and estimated the causal connectivity among core regions involved in preference formation following hard choices. The extent of individuals' choice-induced preference changes were found to be associated with a diminished resting-state excitation between the left dlPFC and the vmPFC, whereas preference consistency was related to a higher resting-state excitation from the ACC to the left hippocampus and vmPFC. Our results point to a model of preference formation during which the dynamic network configurations between left dlPFC, ACC, vmPFC and left hippocampus at rest are linked to preference change or stability.

KEYWORDS

decision-making, dynamic causal modelling, preference formation, resting-state fMRI

1 | INTRODUCTION

Decisions do not only reveal preferences (Rangel, Camerer, & Montague, 2008; Samuelson, 1938)—they also shape them. When people make a hard decisions, that is, choices between equally preferred items, the chosen option typically gains in subjective value, while the rejected alternative loses in subjective value (e.g., Chammat et al., 2017; Izuma et al., 2010; Voigt, Murawski, & Bode, 2017; Voigt, Murawski, Speer, & Bode, 2019). This phenomenon is referred to as choice-induced preference change (reviewed by Izuma & Murayama, 2013; Murayama, Izuma, Aoki, & Matsumoto, 2016). It suggests that preferences are not as rigid as originally assumed but are adapted during the decision-making process (Slovic, 1995).

Until recently, dominant explanations of the choice-induced preference change effect assumed that preferences are adjusted after a choice has been made. The theory of cognitive dissonance (Festinger, 1957) posits that preferences are adjusted at the time of re-evaluation of the options in order to reduce dissonance between preferences (both options are liked equally) and the choice just made (one option was rejected) (Harmon-Jones, Harmon-Jones, & Levy, 2015). In support, neuroimaging studies have found that the dorsal part of the anterior cingulate cortex (ACC) is associated with initial conflict detection between upcoming decisions and existing preferences (i.e. forced to reject an item individuals dislike). It has been proposed that after the initial detection of conflict between upcoming action plans and existing preferences, the dorsolateral

prefrontal cortex (dlPFC) (particularly the left) is involved in the implementation of changes in the underlying neural representation of value, which has been suggested to be encoded in the ventromedial prefrontal cortex (vmPFC) (Izuma et al., 2010). Our recent study was the first to reveal that the left dlPFC was already associated with the implementation of preference changes at the time of making such hard decisions (Voigt et al., 2019). This finding challenges existing explanations, suggesting that preferences are updated 'in the moment' while a hard choice is being made. In addition, there is now strong evidence that memory plays a critical role in preference formation processes (Weilbächer & Gluth, 2016). Choice-induced preference change effects only seem to occur for those items for which decision outcomes are remembered (Chammat et al., 2017; DuBrow, Eberts, & Murty, 2019; Salti, El Karoui, Maillet, & Naccache, 2014; Voigt et al., 2019). This memory-depended change in value has been associated with left hippocampus activity, a core region involved in episodic memory processing (Bird & Burgess, 2008) and vmPFC activity at the time of re-evaluation (Chammat et al., 2017; Voigt et al., 2019). Thus, the left hippocampus might have an important role in representing preferences changes in the longer term. Taken together, these studies suggest that the neural dynamics among ACC, vmPFC, left dlPFC and left hippocampus are critical for choice-induced preference change effects to occur. However, although the dynamic functionality of these brain areas has been confirmed by several studies (e.g., Chammat et al., 2017; Izuma et al., 2010; Mengarelli, Spoglianti, Avenanti, & di Pellegrino, 2015; Voigt et al., 2019), the neural network's effective connectivity remains poorly understood. A better understanding of it would shed further light on its functional relevance for preference changes.

Furthermore, reported findings and effect sizes for the choice-induced preference change effect vary considerably across studies and participants (Chen & Risen, 2010; Izuma et al., 2010; Salti et al., 2014; Voigt et al., 2017). However, no study to date has addressed the origin of these individual differences. One intriguing possibility is that the base reactivity of an individual's neuronal network associated with choice-induced preference change effects is predictive of the strength of the effect in the individual.

The present study asked whether variability in choice-induced preference change effects are partially determined by inter-individual differences in the dynamic organisation of the brain network comprising ACC, vmPFC, left dlPFC and left hippocampus (henceforth referred to as the 'preference formation network'). To this end, we measured resting-state functional magnetic resonance imaging (rsfMRI), which captures low-frequency fluctuations in the blood oxygen level-dependent (BOLD) signal. These fluctuations have been repeatedly shown to explain variation of task-evoked brain activity and behavioural performance in cognitive tasks (Vaidya & Gordon, 2013); for example, resting-state functional connectivity can explain variability in risky choices (Wei et al., 2016), impulsivity (Li et al., 2013) and preference consistency across time (Mackey et al., 2015). However, as resting-state functional connectivity reflects temporal correlations between spatially distant brain signals, this analysis cannot answer questions about causal influences of one brain area over the other. We therefore capitalised on recent advances in modelling the endogenous fluctuations in resting state fMRI data using spectral dynamic causal modelling (spDCM; Friston, Kahan, Biswal, & Razi, 2014). In contrast to functional connectivity analysis, spDCM has the capacity to identify causal (directed) connections between distributed brain areas (i.e. effective connectivity; Friston, Harrison, & Penny, 2003). Resting-state spDCM allows the investigation of multiple neuronal systems simultaneously and has also been shown to be more robust and sensitive to detect individual differences than stochastic DCM (Friston et al., 2014; Razi et al., 2017; Razi, Kahan, Rees, & Friston, 2015). A recent study (Jung et al., 2018) provided evidence that the similarity between baseline effective connectivity during task and during rest was associated with faster reaction times. Investigating brain dynamics in the absence of task stimuli provides knowledge about baseline connectivity patterns, which in turn may relate to behavioural and cognitive manifestations of preference formation and stability. As we aimed to determine whether the future expression of task effects (i.e. choice biases and the tendency to express stability) is—to some extent—already associated with directional connectivity of the preference formation network at rest, spDCM provided an optimal tool to address this research question. We hypothesised that effects related to choice-induced preference change effects relate to changes in the effective connectivity between brain areas known to be involved in the detection of conflict both trigger and implement preference changes (i.e. ACC and vmPFC; left dlPFC and vmPFC, respectively). Consequentially, effects that reflect consistency in preferences instead of a change in preferences might not be associated with pathways triggering and implement changes in the underlying representation of value. These effects might instead be linked to brain regions related to memory for value, such as the vmPFC and left hippocampus (Weilbächer & Gluth, 2016).

2 | MATERIALS AND METHODS

2.1 | Participants

In order to measure the intrinsic causal network dynamics of the preference formation network, resting-state fMRI data was aquired for 22 human participants (13 females; age 18 and 37 years; M = 23.57, *SD* = 4.93). The number of participants was chosen based on a sample size estimation study revealing that 20 participants are sufficient to get reliable DCM predictions (Goulden et al., 2012). Previous research showed that this sample size is sufficient for robust model predictions when applying spDCM to rsfMRI data (Park, Friston, Pae, Park, & Razi, 2018; Preller et al., 2019; Tang, Razi, Friston, & Tang, 2016). All participants were right-handed, English speakers with normal or corrected-to-normal vision, who fasted for 4 hrs prior to the study. No participant had significant health problems (including neurological and psychiatric disorders) or was on psychoactive medication affecting cognitive function or cerebral blood flow. Participants were naïve to the purpose of the study, gave informed consent prior to commencing the experiment and were reimbursed with AUD 60 for their

time. The study was approved by the University of Melbourne Human Research Ethics Committee (no. 1442440) and was conducted according to the Declaration of Helsinki.

2.2 | Experimental procedure

Participants underwent an fMRI session, which was divided into an initial task-free fMRI (i.e. resting-state fMRI) sub-session and a subsequent task-based fMRI session. The results from the fMRI session have been reported previously (Voigt et al., 2019). Because the task-based session succeeded the resting-state MRI session, BOLD signals during the resting state session could not have been modulated by the task (Tambini, Ketz, & Davachi, 2009). The full study protocol of the experiment is outlined in further detail in our previous publication (Voigt et al., 2019), but all relevant sections are reported again below.

2.2.1 | *Task-free* **fMRI** *session*

Participants rested while fixating a central black crosshair (i.e. eyes-open resting-state protocol). Whole-brain images were acquired on a 3 T Siemens MAGNETOM scanner (Erlangen, Germany) with a standard 20-channel head coil (38 axial slices; time of repetition, TR = 2,200 ms; echo time, TE = 30 ms, resolution 3 × 3 × 4 mm with a 1 mm gap). During a total acquisition time of 8.12 min, 220 volumes were acquired for each participant using a single-shot gradient-echo echo-planar imaging (EPI) sequence. In addition, a high-resolution T1-weighted magnetisation-prepared rapid gradient echo (MPRAGE) covering the whole brain was acquired (TR = 1,900 ms; TE = 2.49 ms; T1 = 900 ms; flip angle = 9°; 192 slices; field of view, FOV = 240 mm).

2.2.2 | *Task-based* **fMRI** *session*

In order to assess choice-induced preference changes, following the resting-state fMRI session all participants completed two main tasks: an *incentive-compatible free choice task* (Voigt et al., 2017), followed by a *choice memory task* (Figure 1). Only the behavioural performance of this session will be reported in the present study.

2.2.3 | *The incentive-compatible free-choice task*

The task consisted of four task phases: valuation phase 1, decision phase 1, valuation phase 2 and decision phase 2. Neuroimaging data were acquired during the decision phases and the second valuation phase.

i *Valuation phase 1*. For each trial (292 trials in total), participants indicated how much they were willing to pay (WTP) for a snack food item on a continuum from $0 to $4 within 3 s. Right-handed responses were measured by moving a graphical slider along a continuous valuation scale. All responses were made via an MRI-compatible fibre optic trackball that was controlled by the Curdes' Current Designs 932 interface (www.curdes.com).

ii *Decision phase 1*. A maximum of 80 'hard' and 40 'easy' choice pairs were created, based on the responses of the valuation phase 1, by pairing either items with highly similar (hard) valuations or dissimilar (easy) valuations, respectively. Half of the hard and easy choice pairs (60 total trials) were shown in a pseudo-randomised order, requiring participants to make binary decisions for the item they preferred within a 3 s response window. Participants pressed either the left or right button of a trackball devise to select the choice option that was presented on the left or right of a central fixation cross.

iii *Valuation phase 2*. This task phase was identical to the first valuation phase. Participants were instructed that the purpose was not to probe their memory of the first valuation, but to provide another, independent valuation.

iv *Decision phase 2*. This task phase was identical to the first decision phase except that the remaining half of 60 choice pairs were presented. This allowed us to use the first and second valuations for these items as a control sequence (valuation–valuation–

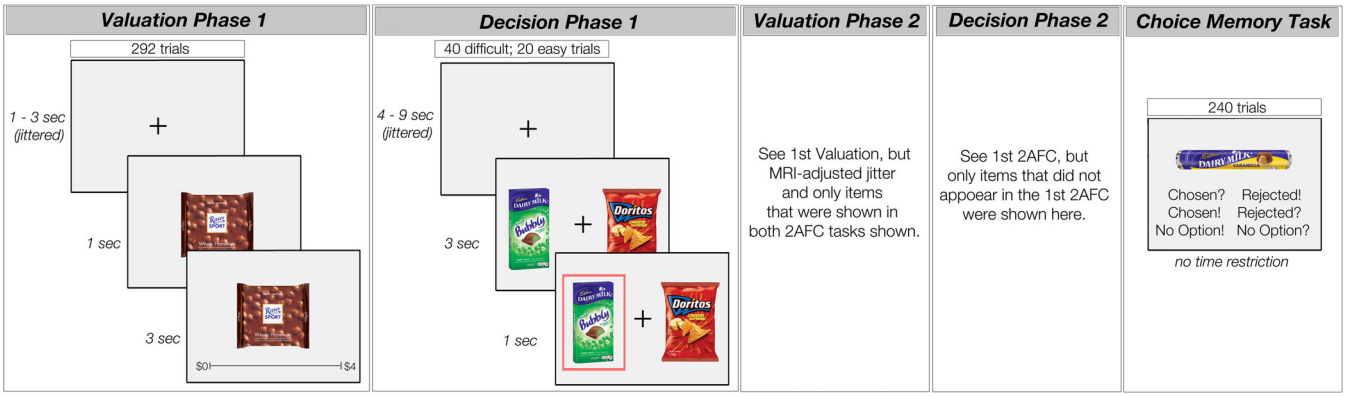

FIGURE 1 The incentivised free-choice task consisted of four consecutive phases (adopted from Voigt et al., 2017): valuation phase 1, decision phase 1, valuation phase 2 and decision phase 2. This task was followed by a choice memory task

choice), assessing changes in valuation that were attributable to regression-to-the-mean effects (Chen & Risen, 2010).

2.2.4 | *The choice memory task*

Participants were presented with the 240 snack food items sequentially and indicated for each whether they remembered having previously chosen or rejected it. Critically, participants were asked to distinguish whether they were absolutely certain (options: Chose! or Rejected!; trials labelled 'remembered'), or whether they felt that they were guessing (Chose? and Rejected?; trials labelled 'guessed') their response.

2.3 | Behavioural data analyses

2.3.1 | Linear mixed effect modelling of behavioural data

Choice-induced preference change effects were assessed via linear mixed effects modelling using the lme4 package (Bates, Mächler, Bolker, & Walker, 2015) in R. The WTP change scores for each individual item were computed by subtracting an item's first WTP values from its second WTP values. Mean-corrected WTP values were used for this subtraction in order to eliminate any variability in WTP indications that were not related to the experimental manipulations. These values were obtained by subtracting the average bid for the respective participant's session from the raw score of each single trial (Voigt et al., 2017).

As choice-induced preference change effects can only be expected for hard decisions (e.g., Izuma et al., 2010; Salti et al., 2014; Sharot, De Martino, & Dolan, 2009; Voigt et al., 2019), the key analyses were conducted for hard decision trials only. The final model was established via backwards elimination of variables by comparing the full starting model to alternatives models based on significant changes in their Bayesian information criterion (BIC) and log-likelihood ratio testing. The Satterthwaite degrees of freedom approximation was used to compute *p*-values.

2.3.2 | *Behavioural outcome measures*

To quantify individual differences in choice-induced preference changes, a *rejection bias*, *choosing bias* and *preference consistency* measure were computed for each participant.

2.3.3 | *Rejection bias*

The rejection bias reflects the degree to which rejection of an item induced a decrease in preferences. The rejection bias was computed by subtracting the (mean-corrected) valuation change (i.e. first WTP values minus second WTP values) following rejection during a hard choice obtained in the experimental control sequence (valuation–valuation–choice) from the (mean-corrected) valuation differential in the intervention sequence (valuation–choice–valuation). Only remembered items were considered, given that reliable choice-induced preference change effects were only found for those items (Chammat et al., 2017; Salti et al., 2014; Voigt et al., 2017). The final scores were multiplied by −1 to ease interpretation, meaning that higher rejection bias scores corresponded to a higher impact of rejection on preference decreases.

2.3.4 | *Choosing bias*

The choosing bias reflects the extent to which choices induced an increase in preferences. The choosing bias was computed by subtracting the valuation change (i.e. mean-corrected first WTP values minus second WTP values for hard choices) following choosing an item during a hard choice obtained in the experimental control sequence (valuation–valuation–choice) from the valuation differential in the intervention sequence (valuation–choice–valuation). Again, only remembered items were considered. Higher choosing scores corresponded to a higher impact of choosing on preference increases.

2.3.5 | *Preference consistency*

In addition to the specific biases, a preference consistency measure was derived, which was not biased by an interspersed choice. The preference consistency score was computed for each participant by calculating the Pearson's correlation coefficient between the WTP values of the first valuation and second valuation in the valuation–valuation–choice condition, because in this condition, the WTP assessments were not biased by a nested choice. As such, this measure indicated the reliability of WTP values for the two subsequent time points.

2.4 | Resting-state fMRI data analysis

2.4.1 | Pre-processing

Functional images were preprocessed using SPM12. The preprocessing steps consisted of slice time correction, realignment, spatial segmentation and normalisation to the standard EPI template of the Montreal Neurological Institute (MNI), and spatial smoothing using a Gaussian kernel of 8 mm FWHM. None of the participants had head motion exceeding 3 mm.

2.4.2 | Region of interest (ROI) selection and time series extraction

Four ROIs were identified as key nodes for effective connectivity analysis, which were based on convergent findings from previous neuroimaging studies investigating the neural correlates of choice-induced

preference changes (Chammat et al., 2017; Izuma et al., 2010; Voigt et al., 2019). The identified neural network comprised of the ACC, the vmPFC, the left dlPFC and left hippocampus (Figure 2a). The MNI coordinates for these regions were based on the functional neuroimaging group findings from the task-based fMRI session with the same participants (Voigt et al., 2019). Specifically, the MNI coordinates for the ACC were identified from the peak voxel activation associated with hard versus easy choices (i.e. decision conflict; MNI −6 26 4), the MNI coordinates for the vmPFC were identified from the peak voxel activation associated with the representation of subjective monetary value (MNI 3 50 −4), the MNI coordinates for the left dlPFC were identified from the peak voxel activation associated with preference changes during the process of making hard choices (MNI −24 5 47) and, finally, the MNI coordinates for the left hippocampus were the identified from peak voxel activation associated with memory-dependent preference changes at the time of re-evaluation (MNI −24 −28 −16).

To extract BOLD fMRI time series corresponding to the aforementioned ROIs (Figure 2b), the pre-processed data were used to establish the residuals of a General Linear Model (GLM). Six head motion parameters and WM/CSF signals were added to the GLM as nuisance regressors. Finally, we selected the MNI coordinates as the centre of a 6-mm sphere to compute the principal eigenvariate and to correct for confounds. As the hippocampus is an anatomically small area relative to the other regions, ROI masks for the hippocampus were created by using a sphere with 6 mm radius around their reported peak voxel activation (in combination with anatomical para- and hippocampal masks from the AAL atlas to ensure that all voxels within the created sphere were within the hippocampal formation). Figure 2a illustrates the location of the four nodes with the corresponding time series.

2.5 | Spectral dynamic causal modelling

The spDCM analyses were performed using the functions of DCM12 (revision 7196) as implemented in SPM12. In order to address our main hypotheses, we focused on spDCM analyses that assessed how

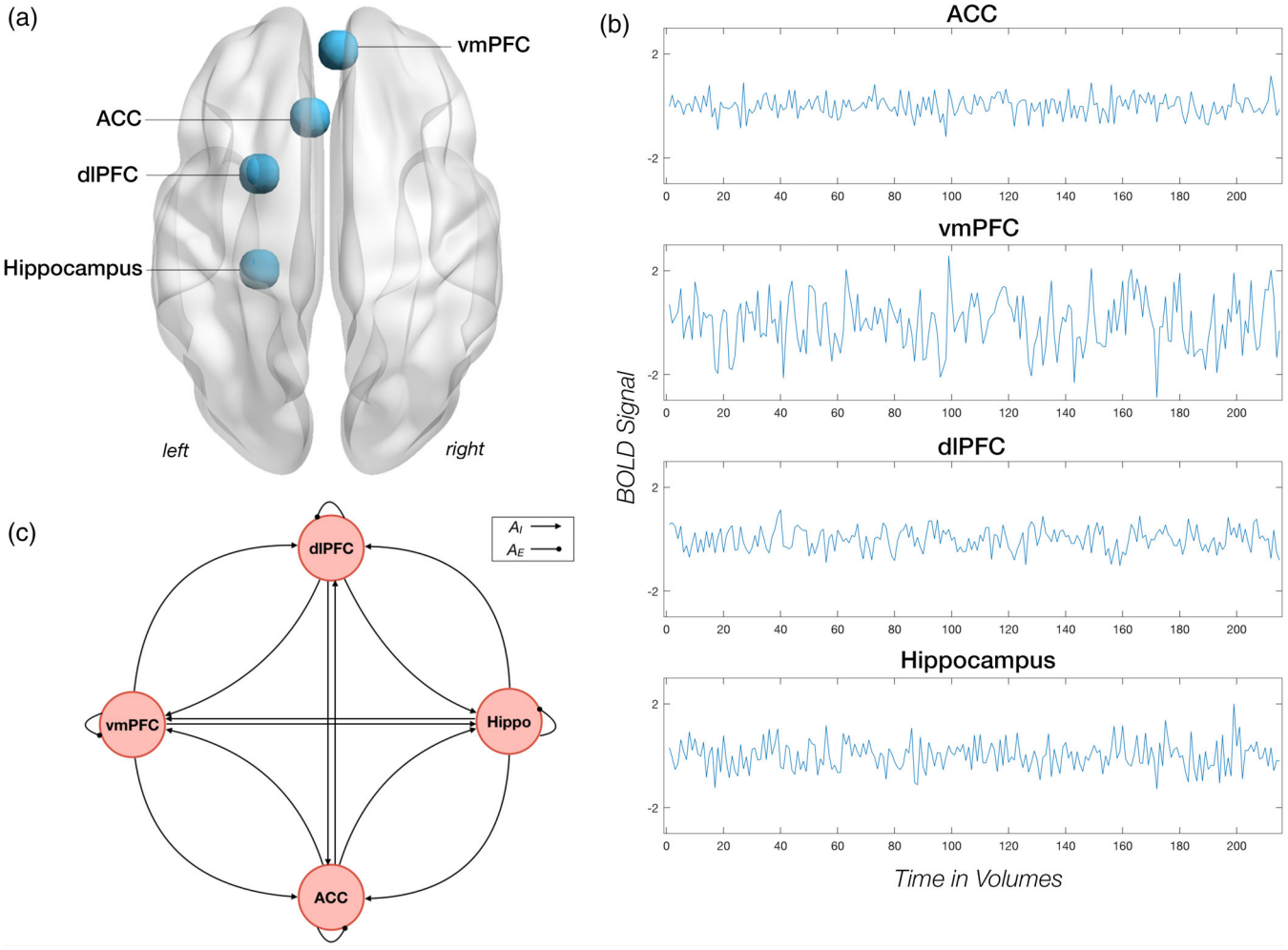

FIGURE 2 (a) The four nodes used in the spectral dynamic causal modelling (spDCM) analyses. The time series from four region of interests (ROIs) were used to invert the spDCMs with the fully connected intrinsic architecture. (b) The time series of the ROIs are shown for a typical subject. (c) The initial model assumed a fully connected intrinsic architecture, comprising of each node's self-inhibition (A_I) and connectivity among each node (A_E) (i.e. 4^2 = 16 parameter model). For abbreviations and MNI coordinates of the ROIs of the spDCM refer to text

changes in effective connectivity in the proposed choice-induced preference formation network were modulated by individuals' (a) rejection bias (RB), (b) choosing bias (CB) and preference consistency (PC).

2.5.1 | First-level spDCM analysis

At the first-level, a fully connected model was created for each participant (i.e. 4^2 = 16 connectivity parameters, including four inhibitory self-connections) (Figure 2c). Next, we inverted (i.e. estimated) the DCMs using spectral DCM, which fits the complex cross-spectral density using a parameterised power-law model of endogenous neuronal fluctuations (Razi et al., 2015). This analysis provides measures of causal interactions between regions, as well as the amplitude of endogenous neuronal fluctuations within each region. Model inversion was based on a variational Laplace procedure (Friston, Mattout, Trujillo-Barreto, Ashburner, & Penny, 2007). This Bayesian inference method uses Free Energy as a proxy for (log) model evidence, while optimising the posterior density under a Laplace approximation of model parameters. After the full spDCM for each participant was estimated, we employed a network discovery procedure using Bayesian model reduction (Friston & Penny, 2011) to find the best model that explained the data.

2.5.2 | Second-level spDCM analyses

To characterise how group differences in neural circuitry were modulated by RB, CB and PC, hierarchical models over the parameters were specified within a hierarchical Parametric Empirical (PEB) framework for DCM (Friston et al., 2016).

2.5.3 | Model 1: Effective connectivity of rejection bias

To investigate the effect of RB on the intrinsic effective connectivity of the preference formation network, the following hierarchical model was estimated within a PEB framework:

$$DCM = b_0 + b_1RB + b_2CB + e$$

RB was modelled as a main regressor of interest, whereas CB was modelled as regressors of no interests.

2.5.4 | Model 2: Effective connectivity of choosing bias

Model 2 was designed to assess how choosing bias, controlling for an individual's rejection bias, affected the neural circuity of the food choice network. CB was modelled as a main regressor of interest, whereas RB was modelled as regressors of no interests.

$$DCM = b_0 + b_1CB + b_2RB + e$$

2.5.5 | Model 3: Effective connectivity of preference consistency

Finally, individuals' preference consistency scores were regressed on the dynamic causal models of each individual's preference formation network. As behavioural analyses have showed that an individual's bias is independent of their choosing or rejection bias (see Results), these scores were not included (see Supporting Information for the description and outcome of Model 4, which includes these as regressors of no interest).

$$DCM = b_0 + b_1PC + e$$

All behavioural parameters were mean-centred to enable that the intercept of each model was interpretable as the mean connectivity. We only report effects (i.e. changes in directed connectivity) that have a posterior probability >0.95. In order to determine the robustness of observed effect sizes, leave-one-out cross-validation was performed. This assesses predictive validity of each model by measuring significant relationships between the model's predictions and observed data.

3 | RESULTS

3.1 | Behavioural results

3.1.1 | Choice-induced preference change effect

Behavioural results revealed a bidirectional memory-depended choice-induced preference change effect (Figure 3a). Choosing between equally valued options increased subsequent WTP values (β = .26, *SE* = 0.10, $p < .05$) and rejecting decreased subsequent WTP values (β = −.17, *SE* = 0.08, $p < .05$). No choice-induced preference effects were observed for easy decisions (i.e. deciding between differently valued items) or when past choice outcomes were guessed or forgotten. Details of these group-level results are reported in a previous article (Voigt et al., 2019).

3.1.2 | Choosing bias and rejection bias

The degree to which choosing and rejecting shaped preferences for remembered choice outcomes varied considerably across individuals (Figure 3b). Fifty-five percent of participants showed an increase of preferences for items that they remembered to have chosen. This bias corresponded to an average increase of \$0.26 (*SD* = \$0.17; ranging from \$0.03 to \$0.52) in the items' WTP bidding scores. The remaining 45% of participants expressed a choosing bias smaller than zero, for which preferences decreased on average \$-0.27 (*SD* = \$0.31; ranging from \$−0.002 to −\$0.86).

Rejecting an item decreased its subsequent value by $0.36 on average (*SD* = $0.19, ranging from $0.01 to $0.83) in 73% of participants. Twenty-seven percent expressed a rejection bias in the opposite direction and their preferences increased, on average by = $0.49 (*SD* = $0.17, ranging from $0.04 to $0.61). In accordance with previous reports (e.g., Salti et al., 2014; Voigt et al., 2017), the effect of rejecting an item's WTP value was nominally larger than the effect of choosing. This difference was, however, not significant ($t[21] = .93$, $p = .36$).

3.1.3 | Preference consistency

There was a strong preference consistency between the two valuation stages of the control sequence in which choice did not bias individuals' WTP scores (M = 0.71, *SD* = 0.22; ranging from 0.12 to 0.95). This finding is consistent with previous reports in which incentive-compatible WTP measures were established as reliable preference assessments (e.g., Voigt et al., 2017, Supplementary Information). There was no significant association between individuals' preference consistency and rejection bias scores (Pearson's $r = .30$, $p = .18$) or choosing bias scores (Pearson's $r = .16$, $p = .47$; Figure 3c).

3.2 | Spectral dynamic causal modelling results

On the subject-level, time-series from ROIs associated with the preference formation network were selected and used to first define and estimate a fully connected DCM for each participant and condition using Variational Laplace (Friston et al., 2007; Figure 1). The average predicted variance by each individuals' final reduced model was very high (M = 96.64, *SD* = 3.70, range = 83.97–99.31), indicating great model convergence (Figure 4 for further diagnostics). Individual connectivity strengths (i.e. first level DCMs) and common connectivity across subjects are presented in Figure SI1 and Figure SI2 in Supporting Information, respectively.

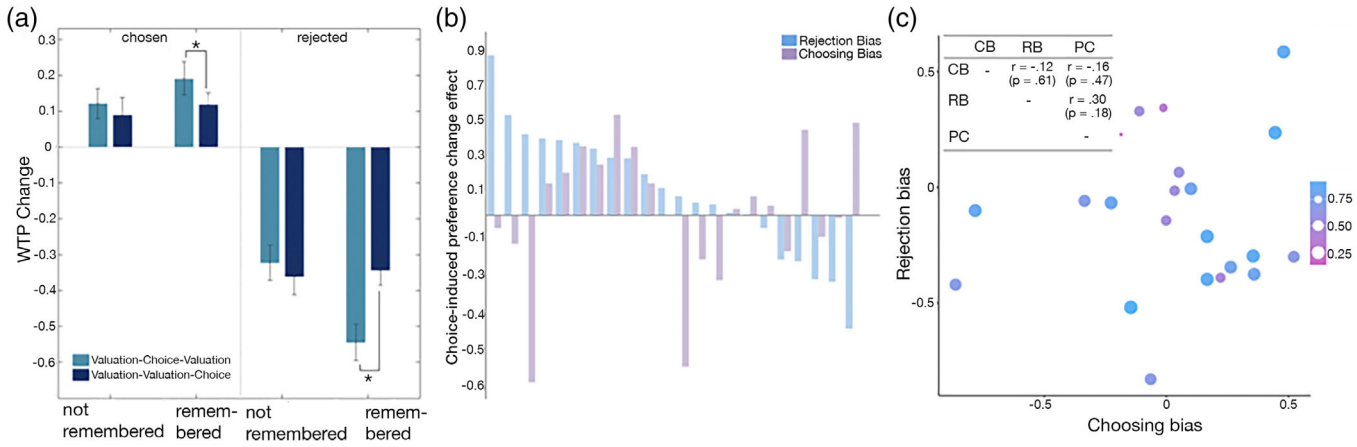

FIGURE 3 (a) The memory-depended, bidirectional choice-induced preference effect. The change in WTP of the intervention sequence, valuation–choice–valuation (turquoise), is contrasted to the WTP change of the control sequence valuation–valuation–choice (blue) (Voigt et al., 2019). (b) The rejecting bias (blue) and choosing bias (purple) for each of all participants. (c) Pearson's bivariate correlations revealed no significant relationship among rejection bias (RB), choosing bias (CB) or preference consistency (PC)

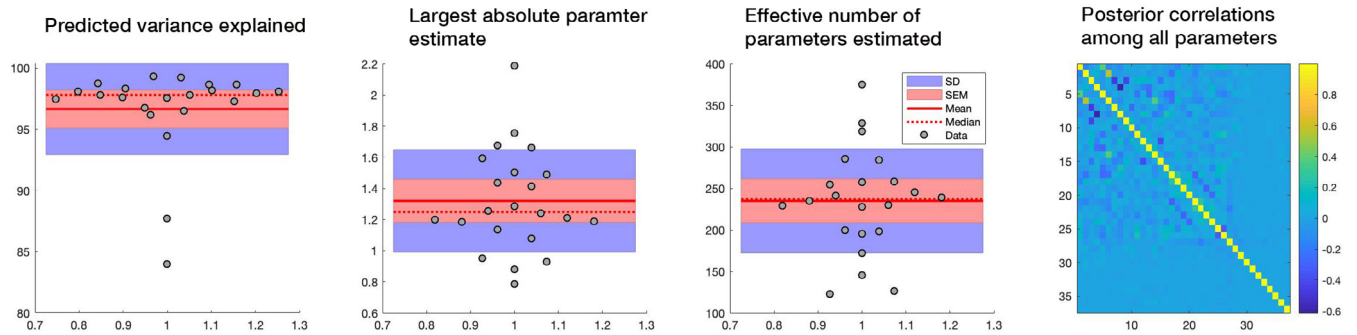

FIGURE 4 First level DCM model convergence statistics indicating good model convergence. (First) Predicted variance explained for each individual were above the minimum threshold of 10% (M = 96.63; *SD* = 3.70). (Second) The largest absolute parameter estimate did not fall below the typical connection strength of 1/8 Hz (M = 1.32; SD = 0.33) (Third). The effective number of parameters are reported in terms of divergence between the posterior and prior densities over parameters (M = 234.95; SD = 62.71. (Fourth) Posterior correlations among all parameters were low, indicating identifiable parameters. All post-hoc diagnostic statistics were obtained via spm_dcm_fmri_check (Zeidman et al., 2019)

3.2.1 | Effective connectivity of rejection bias

Individuals with a higher rejection bias showed a decrease in the excitatory connectivity from ACC to vmPFC (–0.77 Hz, 95% CI [–1.21, –0.33]) and left hippocampus (–0.32 Hz, 95% CI [–0.74, –0.01]), respectively. The excitatory connectivity from the left dlPFC to vmPFC was also reduced in individuals with an increased rejection bias (–0.43 Hz, 95% CI [–0.86, –0.01]). These individuals further showed a higher self-inhibition of ACC (1.07 Hz, 95% CI [0.63, 1.51]) and left hippocampus (0.65 Hz, 95% CI [0.21, 1.09]) and a lower self-inhibition of vmPFC (–0.33 Hz, 95% CI [–0.75, 0.09]). Results are summarised in Table 1 and Figure 5a. Leave-one-out cross-validation revealed that these effects sizes were large enough to predict group effects with an out-of-sample estimate (r = .34, p = .04).

3.2.2 | Effective connectivity of choosing bias

Similar to the rejection bias, a higher choosing bias was associated with decreased excitatory connectivity between left dlPFC and vmPFC, although to a lesser extent (–0.25 Hz, 95% CI [0.15, –0.66]).

TABLE 1 Effective connectivity of rejection bias

	Connectivity	RB relationship	Effect size in Hz (95% CI)
Excitation	ACC → vmPFC	–	–0.77 [–1.21, –0.33]
	dlPFC → vmPFC	–	–0.43 [–0.86, –0.01]
	ACC → Hippo	–	–0.32 [–0.74, 0.10]
Self-inhibition	ACC	+	1.07 [0.63, 1.51]
	vmPFC	–	–0.33 [–0.75, 0.09]
	Hippo	+	0.65 [0.21, 1.09]

Abbreviations: ACC, anterior cingulate cortex; dlPFC, dorsal-lateral prefrontal cortex; Hippo, Hippocampus; RB, Rejection bias; vmPFC, ventro-medial prefrontal cortex.

In terms of self-connections, there was a lower disinhibition of left dlPFC (–0.34 Hz, 95% CI [0.08, –0.78]) and higher disinhibition of the left hippocampus (–0.27 Hz, 95% CI [0.18, –0.71]) in individuals with a higher choosing bias. Results are summarised in Table 2 and Figure 5b. Leave-one-out cross-validation revealed that these effects sizes were not large enough to predict group effects with an out-of-sample estimate (r = .76, p = .86).

3.2.3 | Effective connectivity of preference consistency

Results for preference consistency approximated a reversed effect in comparison to rejection and choosing bias. Specifically, the excitatory projections from ACC to vmPFC (0.80 Hz, 95% CI [0.58, 1.02] and left hippocampus (0.17 Hz, 95%CI [–0.05, 0.38]) were increased in individuals with a higher preference consistency. Further, the excitatory influence of left hippocampus on the vmPFC was enhanced in individuals with a higher preference consistency (0.39 Hz, 95% CI [0.20, 0.62]). The self-inhibition of ACC (–0.63 Hz, 95% CI [–0.84, –0.47]) and left hippocampus (–0.34 Hz, 95% CI [–0.51, –0.17]) decreased with a higher preference consistency. Results are summarised in Table 3 and Figure 5c. Supplementary analyses investigating preference consistency whilst explicitly controlling for preference changes revealed near-identical results. However, in addition to the results original results, a higher dlPFC-vmPFC effective connectivity was found (Figure SI4, Table SI1). Leave-one-out cross-validation revealed that these effects sizes were large enough to predict group effects with an out-of-sample estimate (r = .29, p = .04).

4 | DISCUSSION

In utilising recent advances in modelling the endogenous low-frequency fluctuations in the rsfMRI BOLD signal (Friston et al., 2014;

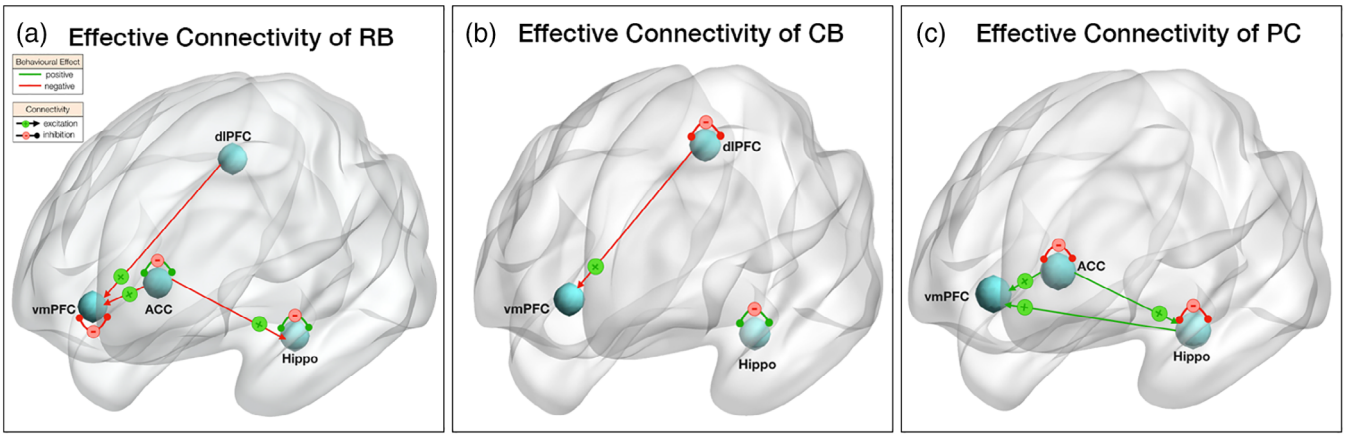

FIGURE 5 Spectral dynamic causal modelling results. Green/red arrows indicate a positive/negative relationship with the respective behavioural measure. Plus/negative sign indicates excitation/inhibition of connection. CB, choosing bias; PC, preference consistency; RB, rejection bias

TABLE 2 Effective connectivity of choosing bias

	Connection	CB relationship	Effect size in Hz (95% CI)
Excitation	dlPFC → vmPFC	–	−0.25 [0.15, −0.66]
Self-inhibition	dlPFC	–	−0.34 [0.08, −0.78]
	Hippo	+	−0.27 [0.18, −0.71]

Abbreviations: CB, Choosing bias; dlPFC, dorsal-lateral prefrontal cortex; Hippo, hippocampus; vmPFC, ventro-medial prefrontal cortex.

TABLE 3 Effective connectivity of preference consistency

	Connection	PC relationship	Effect size in Hz (95% CI)
Excitation	ACC → vmPFC	+	0.80 [0.58, 1.02]
	ACC → Hippo	+	0.17 [−0.05, 0.38]
	Hippo → vmPFC	+	0.39 [0.20, 0.62]
Self-inhibition	ACC	–	−0.63 [−0.84, −0.47]
	Hippo	–	−0.34 [−0.51, −0.17]

Abbreviations: ACC, anterior cingulate cortex; Hippo, hippocampus; PC, preference consistency; vmPFC, ventro-medial prefrontal cortex.

Park et al., 2018), the present study is the first to reveal the underlying causal network dynamics associated with individuals' preference formation and stability scores. We recently provided evidence that choice-induced preference change effects can already be explained by activation during the choice phase itself, that is, before an active, explicit re-evaluation takes place. Our resting-state analysis approach allowed us to look back even further and explore factors that might moderate this effect before participants even made choices: We hypothesised that the initial intrinsic causal dynamics in the very same neural network that were associated with task-related effects during choice might already explain parts of the effect's variance. In other words, we aimed to understand whether the connectivity dynamics might play a role in participants' susceptibility for expressing such biases (or preference stability) before being in a decision situation. Our results show that individuals with higher choice-induced preference changes had a diminished influence of areas involved in cognitive control (i.e. left dlPFC and ACC) on regions computing decision value and recalling memory of past choices (i.e. vmPFC and left hippocampus). The network dynamics showed a reversed dynamic in scenarios in which the decision context did not prompt a change in preferences, but individuals relied on previously learned values (i.e. preference consistency). These results indicate that the strength of the expression of choice-induced preference change and preference consistency effects was partly determined by inter-individual differences in the brain's intrinsic effective connectivity architecture. Moreover, our results point to a model of preference formation in which the dynamic communication among ACC, left dlPFC, vmPFC, and left hippocampus at rest might be linked to an individual's ability to flexibly adapt their preferences depending on the decision context. Regarding the proposed mechanisms, we note, however, that the relationship between task-based and resting-state effective connectivity and its behavioural correlates remains elusive. The inter-individual variations in effective connectivity do not necessarily overlap with the inter-individual variations in effective connectivity during task performance (Fox & Raichle, 2007; Jung et al., 2018). In other words, our study cannot determine conclusively whether the individual differences in preference formation associated with the resting-state network dynamics are identical to the network dynamics that would have been observed during task. At this stage, only one study has investigated the relationship between effective connectivity for resting and task states and their relation to behaviour (Jung et al., 2018). The authors found that when task-related increases in connectivity correlated with the intrinsic connectivity in their memory task, or intrinsic connectivity increased during resting state, processing speed was slower. This means that when effective connectivity for the task was less similar to connectivity at rest, participants showed faster response times. Future studies are needed to address whether the resting-state dynamics revealed in our study are also engaged during task performance and how potential deviations might translate to differences in behavioural performance.

Our behavioural results show that choosing and rejection biases were not expressed evenly across participants. Whereas the majority of our participants expressed decreasing preferences after rejecting items, only slightly more than half of the sample showed preference increases after choosing items. These individual differences are in line with recent research reporting stronger average rejection bias effects compared to choosing bias effects (e.g., Izuma et al., 2010; Salti et al., 2014; Sharot et al., 2009; Voigt et al., 2017). One explanation for why rejecting ('losing') an option might have a larger impact than choosing ('gaining') an option on future preferences might be related to loss aversion, the effect of losses looming larger than gains (Kahneman & Tversky, 1979). It is therefore possible that rejecting/losing is more emotionally salient than choosing/gaining (Sokol-Hessner & Rutledge, 2019), leading to stronger memory traces of the former when updating preferences. Regarding preference consistency, we replicated findings of our earlier study showing that individuals showed a high consistency in their preferences, confirming that incentive-compatible preference (i.e. WTP) assessments were reliable (Voigt et al., 2017). To explain the behavioural differences in choice biases and preference consistency, we assumed that these did not simply reflect noise, but that they might (at least to some extent) be meaningful. Our spDCM analyses explored whether and how the intrinsic causal dynamics of the neural network underlying adaptive preference changes during hard decisions (i.e. ACC, left dlPFC, vmPFC and left hippocampus; Chammat et al., 2017; Izuma et al., 2010; Voigt et al., 2019), and we found that it explained a significant fraction of the observed behavioural variability.

Our spDCM results showed that the smaller the impact of brain areas involved in the computation of self-controlled choice (i.e. ACC and left dlPFC) on regions associated with the computation and representation of preferences (i.e. vmPFC and left hippocampus), the higher the choice-induced preference change effect was. Specifically, there was reduced resting-state excitatory connectivity from left dlPFC to

vmPFC as well as from ACC to vmPFC and left hippocampus in individuals with a higher rejection bias as well as in individuals with a higher choosing biases. A weaker resting-state excitation from the dlPFC to the vmPFC might facilitate the rapid generation of new choice-related value signals, instead of incorporating these with previous value representations in the vmPFC, which might explain the association with higher rejection biases. Our task-based fMRI results are in support of this conjuncture, showing that left dlPFC was associated with rapid preference changes during the process of deciding between equally valued alternatives (Voigt et al., 2019), whereby vmPFC activity has been associated with continuous encoding of value representations after the choice (Izuma et al., 2010; Sharot et al., 2009). Other studies revealed that vmPFC and dlPFC compute value (Hare, Hakimi, & Rangel, 2014; Rudorf & Hare, 2014); however, value computation was lagged in vmPFC compared to dlPFC (Baumgartner, Knoch, Hotz, Eisenegger, & Fehr, 2011; Hare, Camerer, & Rangel, 2009). Given dlPFC's rich reciprocal connections to motor areas, this area has been shown to be involved in generating motoric response components related to the choice (MacDonald, Cohen, Stenger, & Carter, 2000). Previous studies further linked dlPFC-vmPFC effective connectivity to controlled, regulated decision-making (Hare et al., 2009) and context-specific attribute valuation (Rudorf & Hare, 2014), in which dlPFC modulates the value-computations in vmPFC by integrating choice attributes according to current behavioural goals. In the context of our results, this could mean that lower excitation between these regions could give dlPFC a stronger weight when executing the decision and hence a stronger role in constructing the new value during choice. Higher excitation between left dlPFC and vmPFC, on the other hand, might lead to more closely integrated updating, with an additional strong weight on the previous value representation, leading to smaller updates (and hence smaller choice biases). In support, we found that the excitation at rest between left dlPFC and vmPFC was less reduced for choosing biases as opposed to rejection biases, which might be a possible baseline neuronal correlate of the finding that behaviourally the rejection bias was on average more pronounced than the choosing bias in our and previous studies. Supplementary analyses investigating preference consistency whilst controlling for preference changes revealed near-identical results. The only difference was that in addition, a higher dlPFC-vmPFC effective connectivity was found, which further strengthens this conclusion.

In scenarios in which individuals were required to access memorised item values, our results revealed a stronger resting-state excitation of the left hippocampus on vmPFC. Previous studies showed that left hippocampus activity (Chammat et al., 2017; Voigt et al., 2019), as well as its functional (Ross, LoPresti, Schon, & Stern, 2013; Wimmer, Li, Gorgolewski, & Poldrack, 2018) and effective connectivity (Gluth, Sommer, Rieskamp, & Büchel, 2015) to the vmPFC, play an essential role in memory-guided decision-making. The hippocampus itself is a core area involved in encoding and retrieval of memories (Bird & Burgess, 2008). Although, as previously noted, we cannot directly elucidate whether these task-based results directly translate to our findings of resting-state networks, it is possible that the increased resting-state excitation from the left hippocampus on vmPFC might facilitate the integration of memory on value computation processes, explaining the improved ability for remembering and accessing memories of past value-based choices. Our results further reveal that preference consistency was associated with an increased resting-state excitation from ACC to vmPFC as well as left hippocampus, which is the opposite direction to rejection biases. As this triangular resting-state network (i.e. ACC, vmPFC and left hippocampus) was found for rejection biases and for preference consistency, it might reflect a facilitation top-down cognitive control mechanism that mediates the impact of irrational contextual biases. If preference consistency is required, this mechanism is enhanced (as reflected by increased excitatory connectivity within the network), enabling the individual to eliminate the impact of contextual biases. However, in the case of difficult decision scenarios, this mechanism is tuned down (as indicated by decreased excitation within the triangular network), which might assist the individual to use choice history biases for updating value, which could in turn enable the individual to facilitate the decision process (Voigt et al., 2019).

Taken together, our study is the first to reveal how resting-state dynamics within the preference formation network relate to preference formation and stability. Preference changes and stability relate to opposite resting-state network dynamics of areas involved in memory and value processing. Of course, our results do not directly speak to the specific roles of these regions in the cognitive processes of interest. However, it is reasonable to speculate that brain areas involved in memory and value processing need to work in tandem to enable the individual to change (if a change in preferences is indicated as in hard decision scenarios) or to remain consistent (if no change in cognitive representation is required, e.g., in two subsequent valuation assessments). For hard decisions, preferences might be updated online as early as during the process of making decisions (Voigt et al., 2019), and these online updates, which become behaviourally relevant in the long-term, are also more efficiently stored in episodic memory. While our study is only the first step in deriving an understanding of this interplay of brain regions at rest and how this might translate into the expression of the behavioural effects, complementary future task-based studies will be required to examine how the revealed resting-state network dynamics are related to network dynamics during task performance.

ACKNOWLEDGMENTS

The authors thank Adeel Razi for valuable discussions; Sophia Bock, William Turner and Richard McIntyre for support with MRI data acquisition. This study was supported by an Australian Research Council Discovery Early Career Researcher Award (DE 140100350) to S.B.

CONFLICT OF INTEREST

The authors declare no conflict of interest.

DATA AVAILABILITY STATEMENT

The data that support the findings of this study are available from the corresponding author upon reasonable request.

ORCID

Katharina Voigt https://orcid.org/0000-0002-1027-9223

REFERENCES

Bates, D., Mächler, M., Bolker, B., & Walker, S. (2015). Fitting linear mixed-effects models using lme4. *Journal of Statistical Software*, *67*(1), 1–48. https://doi.org/10.18637/jss.v067.i01

Baumgartner, T., Knoch, D., Hotz, P., Eisenegger, C., & Fehr, E. (2011). Dorsolateral and ventromedial prefrontal cortex orchestrate normative choice. *Nature Neuroscience*, *14*(11), 1468–1474. https://doi.org/10.1038/nn.2933

Bird, C. M., & Burgess, N. (2008). The hippocampus and memory: Insights from spatial processing. *Nature Reviews Neuroscience*, *9*(3), 182–194. https://doi.org/10.1038/nrn2335

Chammat, M., Karoui, I. E., Allali, S., Hagège, J., Lehongre, K., Hasboun, D., … Naccache, L. (2017). Cognitive dissonance resolution depends on episodic memory. *Scientific Reports*, *7*: 41320. https://doi.org/10.1038/srep41320

Chen, M. K., & Risen, J. L. (2010). How choice affects and reflects preferences: Revisiting the free-choice paradigm. *Journal of Personality and Social Psychology*, *99*(4), 573–594. https://doi.org/10.1037/a0020217

DuBrow, S., Eberts, E. A., & Murty, V. P. (2019). A common mechanism underlying choice's influence on preference and memory. *Psychonomic Bulletin & Review*, *26*(6), 1958–1966. https://doi.org/10.3758/s13423-019-01650-5

Festinger, L. (1957). *A theory of cognitive dissonance*. New York: Row, Peterson & Co.

Fox, M. D., & Raichle, M. E. (2007). Spontaneous fluctuations in brain activity observed with functional magnetic resonance imaging. *Nature Reviews Neuroscience*, *8*(9), 700–711. https://doi.org/10.1038/nrn2201

Friston, K., Harrison, L., & Penny, W. (2003). Dynamic causal modelling. *NeuroImage*, *19*(4), 97–109.

Friston, K., Kahan, J., Biswal, B., & Razi, A. (2014). A DCM for resting state fMRI. *NeuroImage*, *94*, 396–407.

Friston, K., Mattout, J., Trujillo-Barreto, N., Ashburner, J., & Penny, W. (2007). Variational free energy and the Laplace approximation. *NeuroImage*, *34*(1), 220–234. https://doi.org/10.1016/j.neuroimage.2006.08.035

Friston, K., & Penny, W. (2011). Post hoc Bayesian model selection. *NeuroImage*, *56*(4), 2089–2099. https://doi.org/10.1016/j.neuroimage.2011.03.062

Friston, K. J., Litvak, V., Oswal, A., Razi, A., Stephan, K. E., van Wijk, B. C. M., … Zeidman, P. (2016). Bayesian model reduction and empirical Bayes for group (DCM) studies. *NeuroImage*, *128*, 413–431. https://doi.org/10.1016/j.neuroimage.2015.11.015

Gluth, S., Sommer, T., Rieskamp, J., & Büchel, C. (2015). Effective connectivity between hippocampus and ventromedial prefrontal cortex controls preferential choices from memory. *Neuron*, *86*(4), 1078–1090. https://doi.org/10.1016/j.neuron.2015.04.023

Goulden, N., Elliott, R., Suckling, J., Williams, S. R., Deakin, J. F. W., & McKie, S. (2012). Sample size estimation for comparing parameters using dynamic causal modeling. *Brain Connectivity*, *2*(2), 80–90. https://doi.org/10.1089/brain.2011.0057

Hare, T. A., Camerer, C. F., & Rangel, A. (2009). Self-control in decision-making involves modulation of the vmPFC valuation system. *Science*, *324*(5927), 646–648. https://doi.org/10.1126/science.1168450

Hare, T. A., Hakimi, S., & Rangel, A. (2014). Activity in dlPFC and its effective connectivity to vmPFC are associated with temporal discounting. *Frontiers in Neuroscience*, *8*:50. https://doi.org/10.3389/fnins.2014.00050

Harmon-Jones, E., Harmon-Jones, C., & Levy, N. (2015). An action-based model of cognitive-dissonance processes. *Current Directions in Psychological Science*, *24*(3), 184–189. https://doi.org/10.1177/0963721414566449

Izuma, K., Matsumoto, M., Murayama, K., Samejima, K., Sadato, N., & Matsumoto, K. (2010). Neural correlates of cognitive dissonance and choice-induced preference change. *Proceedings of the National Academy of Sciences*, *107*(51), 22014–22019. https://doi.org/10.1073/pnas.1011879108

Izuma, K., & Murayama, K. (2013). Choice-induced preference change in the free-choice paradigm: A critical methodological review. *Frontiers in Psychology*, *4*:41.

Jung, K., Friston, K. J., Pae, C., Choi, H. H., Tak, S., Choi, Y. K., … Park, H.-J. (2018). Effective connectivity during working memory and resting states: A DCM study. *NeuroImage*, *169*, 485–495. https://doi.org/10.1016/j.neuroimage.2017.12.067

Kahneman, D., & Tversky, A. (1979). Prospect theory: An analysis of decision under risk. *Econometrica*, *47*(2), 263–292. https://doi.org/10.2307/1914185

Li, N., Ma, N., Liu, Y., He, X.-S., Sun, D. L., & Fu, X. M. (2013). Resting-state functional connectivity predicts impulsivity in economic decision-making. *The Journal of Neuroscience*, *33*(11), 4886–4895.

MacDonald, A. W., Cohen, J. D., Stenger, V. A., & Carter, C. S. (2000). Dissociating the role of the dorsolateral prefrontal and anterior cingulate cortex in cognitive control. *Science*, *288*(5472), 1835–1838. https://doi.org/10.1126/science.288.5472.1835

Mackey, S., Olafsson, V., Aupperle, R., Lu, K., Fonzo, G. A., Parnass, J., … Paulus, M. P. (2015). Greater preference consistency during the Willingness-to-Pay task is related to higher resting state connectivity between the ventromedial prefrontal cortex and the ventral striatum. *Brain Imaging and Behaviour*, *10*(3), 730–738.

Mengarelli, F., Spoglianti, S., Avenanti, A., & di Pellegrino, G. (2015). Cathodal tDCS over the left prefrontal cortex diminishes choice-induced preference change. *Cerebral Cortex*, *25*(5), 1219–1227. https://doi.org/10.1093/cercor/bht314

Murayama, K., Izuma, K., Aoki, R., & Matsumoto, K. (2016). "Your choice" motivates you in the brain: The emergence of autonomy neuroscience. In *Advances in motivation and achievement* (pp. 95–125). Bingley, England: Emerald Group Publishing Limited. https://doi.org/10.1108/S0749-742320160000019004

Park, H.-J., Friston, K. J., Pae, C., Park, B., & Razi, A. (2018). Dynamic effective connectivity in resting state fMRI. *NeuroImage*, *180*, 594–608. https://doi.org/10.1016/j.neuroimage.2017.11.033

Preller, K. H., Razi, A., Zeidman, P., Stämpfli, P., Friston, K. J., & Vollenweider, F. X. (2019). Effective connectivity changes in LSD-induced altered states of consciousness in humans. *Proceedings of the National Academy of Sciences*, *116*(7), 2743–2748. https://doi.org/10.1073/pnas.1815129116

Rangel, A., Camerer, C., & Montague, P. R. (2008). A framework for studying the neurobiology of value-based decision making. *Nature Reviews Neuroscience*, *9*(7), 545–556. https://doi.org/10.1038/nrn2357

Razi, A., Kahan, J., Rees, G., & Friston, K. J. (2015). Construct validation of a DCM for resting state fMRI. *NeuroImage*, *106*, 1–14. https://doi.org/10.1016/j.neuroimage.2014.11.027

Razi, A., Seghier, M. L., Zhou, Y., McColgan, P., Zeidman, P., Park, H.-J., … Friston, K. J. (2017). Large-scale DCMs for resting-state fMRI. *Network Neuroscience*, *1*(3), 222–241. https://doi.org/10.1162/NETN_a_00015

Ross, R. S., LoPresti, M. L., Schon, K., & Stern, C. E. (2013). Role of the hippocampus and orbitofrontal cortex during the disambiguation of social cues in working memory. *Cognitive, Affective, & Behavioral Neuroscience*, *13*(4), 900–915. https://doi.org/10.3758/s13415-013-0170-x

Rudorf, S., & Hare, T. A. (2014). Interactions between dorsolateral and ventromedial prefrontal cortex underlie context-dependent stimulus valuation in goal-directed choice. *The Journal of Neuroscience*, *34*(48), 15988–15996. https://doi.org/10.1523/JNEUROSCI.3192-14.2014

Salti, M., El Karoui, I., Maillet, M., & Naccache, L. (2014). Cognitive dissonance resolution is related to episodic memory. *PLoS One*, *9*(9): e108579. https://doi.org/10.1371/journal.pone.0108579

Samuelson, P. A. (1938). A note on pure theory of consumer's behaviour. *Economica*, *5*(17), 61–71.

Sharot, T., De Martino, B., & Dolan, R. J. (2009). How choice reveals and shapes expected hedonic outcome. *Journal of Neuroscience*, *29*(12), 3760–3765. https://doi.org/10.1523/JNEUROSCI.4972-08.2009

Slovic, P. (1995). The construction of preference. *American Psychologist*, *50* (5), 364–371.

Sokol-Hessner, P., & Rutledge, R. B. (2019). The psychological and neural basis of loss aversion. *Current Directions in Psychological Science*, *28*(1), 20–27. https://doi.org/10.1177/0963721418806510

Tambini, A., Ketz, N., & Davachi, L. (2009). Enhanced brain correlations during rest are related to memory for recent experiences. *Neuron*, *65*, 280–290.

Tang, R., Razi, A., Friston, K. J., & Tang, Y.-Y. (2016). Mapping smoking addiction using effective connectivity analysis. *Frontiers in Human Neuroscience*, *10*: 195. https://doi.org/10.3389/fnhum.2016.00195

Vaidya, C. J., & Gordon, E. M. (2013). Phenotypic variability in resting-state functional connectivity: Current status. *Brain Connectivity*, *3*(2), 99–120. https://doi.org/10.1089/brain.2012.0110

Voigt, K., Murawski, C., & Bode, S. (2017). Endogenous formation of preferences: Choices systematically change willingness-to-pay for goods. *Journal of Experimental Psychology: Learning, Memory, and Cognition*, *43* (12), 1872–1882. https://doi.org/10.1037/xlm0000415

Voigt, K., Murawski, C., Speer, S., & Bode, S. (2019). Hard decisions shape the neural coding of preferences. *The Journal of Neuroscience*, *39*(4), 718–726. https://doi.org/10.1523/JNEUROSCI.1681-18.2018

Wei, Z., Yang, N., Liu, Y., Wang, Y., Han, L., Zha, R., … Zhang, X. (2016). Resting-state functional connectivity between the dorsal anterior cingulate cortex and thalamus is associated with risky decision-making in nicotine addicts. *Scientific Reports*, *6*:21778.

Weilbächer, R., & Gluth, S. (2016). The interplay of hippocampus and ventromedial prefrontal cortex in memory-based decision making. *Brain Sciences*, *7*(1), E4. https://doi.org/10.3390/brainsci7010004

Wimmer, G. E., Li, J. K., Gorgolewski, K. J., & Poldrack, R. A. (2018). Reward learning over weeks versus minutes increases the neural representation of value in the human brain. *The Journal of Neuroscience*, *38*(35), 7649–7666. https://doi.org/10.1523/JNEUROSCI.0075-18.2018

Zeidman, P., Jafarian, A., Corbin, N., Seghier, M. L., Razi, A., Price, C. J., & Friston, K. J. (2019). A guide to group effective connectivity analysis, part 1: First level analysis with DCM for fMRI. *NeuroImage*, *200*, 174–190. https://doi.org/10.1016/j.neuroimage.2019.06.031

SUPPORTING INFORMATION

Additional supporting information may be found online in the Supporting Information section at the end of this article.

How to cite this article: Voigt K, Murawski C, Speer S, Bode S. Effective brain connectivity at rest is associated with choice-induced preference formation. *Hum Brain Mapp*. 2020;1–12. https://doi.org/10.1002/hbm.24999